Ocean Dynamics (2009) 59:433–449
DOI 10.1007/s10236-008-0161-6

Regional patterns of observed sea level change: insights from a 1/4° global ocean/sea-ice hindcast

Alix Lombard · Gilles Garric · Thierry Penduff

Received: 9 November 2007 / Accepted: 20 October 2008 / Published online: 26 November 2008

Abstract A global eddy-admitting ocean/sea-ice simulation driven over 1958–2004 by daily atmospheric forcing is used to evaluate spatial patterns of sea level change between 1993 and 2001. In the present study, no data assimilation is performed. The model is based on the Nucleus for European Models of the Ocean code at the 1/4° resolution, and the simulation was performed without data assimilation by the DRAKKAR project. We show that this simulation correctly reproduces the observed regional sea level trend patterns computed using satellite altimetry data over 1993–2001. Generally, we find that regional sea level change is best simulated in the tropical band and northern oceans, whereas the Southern Ocean is poorly simulated. We examine the respective contributions of steric and bottom pressure changes to the total regional sea level changes. For the steric component, we analyze separately the contributions of temperature and salinity changes as well as upper and lower ocean contributions. Generally, the model results show that most regional sea level changes arise from temperature changes in the upper 750 m of the ocean. However, contributions of salinity changes and deep steric changes can be locally important. We also propose a map of ocean bottom pressure changes. Finally, we assess the robustness of such a model by comparing this simulation with a second simulation performed by MERCATOR-Ocean based on the same core model, but differing by its short length of integration (1992–2001) and its surface forcing data set. The long simulation presents better performance over 1993–2001 than the short simulation, especially in the Southern Ocean where a long adjustment time seems to be needed.

Keywords Regional sea level change · Eddy-admitting ocean model · Altimetry observations

Responsible editor: Anthony C. Hirst

In memory of my little brother Jean-Eudes, whose thirst for science filled out the rich discussions we had about my investigations and his job as user-service provider for MERCATOR-Ocean.

A. Lombard (✉)
CNES,
18 Avenue Edouard Belin,
31 401, Toulouse Cedex 9, France
e-mail: Alix.Lombard@cnes.fr

G. Garric
MGC/MERCATOR-Ocean,
8–10 rue Hermès, Parc Technologique du Canal,
31520, Ramonville-St-Agne, France

T. Penduff
MEOM-LEGI,
Laboratoire des Ecoulements Géophysiques et Industriels,
CNRS, UJF, INPG, BP53,
38041, Grenoble Cedex 9, France

1 Introduction

Recent studies based on satellite altimetry observations have shown that the sea level is rising at a global mean rate of about 3 mm/year since the beginning of the 1990s (Lombard et al. 2006). However, this rise is not uniform: in some regions (e.g., Western Pacific ocean), the rise reaches several times the global mean sea level rise, while in other regions (e.g., Eastern Pacific ocean), the sea level has been falling. Many recent studies (Cabanes et al. 2001; Willis et al. 2004; Lombard et al. 2006) have shown that spatial patterns of sea level change is mainly due to thermal expansion of the upper 700 m of the ocean, computed using global in situ temperature observations (Willis et al. 2004; Guinehut et al. 2004; Levitus et al. 2005; Ishii et al. 2006).

However, mechanisms of heat distribution within the ocean are not yet fully understood and other processes can contribute to spatial patterns of sea level change (e.g., local salinity change or redistribution of mass by the ocean circulation). The topic addressed in this study is of considerable interest: Are we able to reproduce past regional sea level trends using pure forced global ocean model simulations without data assimilation? Can we give some physical insight into the physical mechanisms responsible for this regional distribution of sea level change? These are the two main questions we intend to answer in the present study.

For that purpose, we analyze the numerical outputs of a forced global ocean model (the Nucleus for European Models of the Ocean [NEMO] model, in its global 1/4° "eddy-admitting" version) without any data assimilation to study the spatial patterns of sea level change and compare the model results with sea level observations from Topex/Poseidon (T/P) satellite altimetry.

The simulation used (hereafter, the "long-DRAKKAR" simulation) was implemented over 1958–2004 in the context of the DRAKKAR project (http://www.ifremer.fr/lpo/drakkar).

In the last part of the paper, we analyze a second simulation of the same model, but with a short spin-up and slightly different surface forcing (hereafter, the "short-MERCATOR" simulation) that was implemented over 1993–2001 by MERCATOR-Ocean (http://www.mercator-ocean.fr).

2 Model description

2.1 Common features of long-DRAKKAR and short-MERCATOR simulations

The global long-DRAKKAR and short-MERCATOR models are based on the same primitive equation (with Boussinesq and hydrostatic approximations), free surface ocean circulation model NEMO which presently includes the latest version of OPA9 (Madec et al. 1998). Both configurations have a 1/4° horizontal resolution. Both configurations use the "partial steps" (Adcroft et al. 1997) topography represented as staircases but making the depth of the bottom cell variable and adjustable to the real depth of the ocean floor. For a complete description of the model physics and potential, please refer to Barnier et al. (2006). Both configurations use a coupled thermodynamic–dynamic sea-ice model Louvain sea-ice model 2 (Fichefet and Maqueda 1997; Goosse and Fichefet 1999).

In both simulations, a relaxation of sea surface salinity (hereafter, SSS) is applied toward the Levitus et al. (2005) monthly climatology. The relaxation time scales, given for a mixed layer of 40 m depth, are similar for the long-DRAKKAR run (240 days in open ocean and 48 days under sea-ice) and the short-MERCATOR run (160 days everywhere), except under sea-ice. Note that this relaxation of SSS is only performed at the surface. Its impact is negligible at low and mid latitudes, but could be important at high latitude (especially on halosteric trends, see Section 3) and explain some of the differences between both simulations (see Section 4). Finally, a monthly climatology of river runoff (Dai and Trenberth 2002) is taken into account in the water budget (1.2 Sv).

2.2 Major differences between the two simulations

2.2.1 Long-DRAKKAR

Long-DRAKKAR uses 46 vertical levels (intervals of 6 m in surface layers increasing to 250 m in deep layers). This simulation is driven by the hybrid DRAKKAR forcing set 3 (DFS3) surface forcing function described in Brodeau et al. (2007) where turbulent fluxes are computed from six hourly ERA40 atmospheric variables using bulk formulae proposed by Large and Yeager (2004). A modification is made to the wind forcing to improve the representation of the katabatic winds around Antarctica (Mathiot et al. 2005). Daily radiation fluxes and monthly precipitations are adapted from the coordinated ocean reference experiments (CORE) dataset assembled by Large and Yeager (2004).

The experiment was started from rest on January 1, 1958 with initial conditions for temperature and salinity derived from the Levitus et al. (2005) climatology at mid and low latitudes, the PHC2.1 and MEDATLAS climatologies in the Arctic Ocean and the Mediterranean Sea, respectively (see Barnier et al. 2006 and references herein for more details), and integrated until 2004.

2.2.2 Short-MERCATOR

This configuration uses 50 vertical levels (intervals of 1 m in surface layers increasing to 450 m in deep layers). Daily surface atmospheric conditions are given by the European Centre for Medium-Range Weather Forecast (ECMWF) reanalysis project ERA40. The surface atmospheric forcing fluxes are calculated using the empirical bulk parameterization described by Goose et al. (2001). A mean correction is applied to the tropical ECMWF rainfall flux in order to close the global freshwater budget (precipitation − evaporation + runoff) at the surface for the whole period.

Briefly, this method consists in assuming that (1) the ECMWF precipitation field should conform to the observed precipitation field in the tropics [the GPCPv2 dataset from Huffman et al. (1997) for our purpose]; (2) the water budget, precipitation minus evaporation (calculated by the model in our case) has to be zero in a global sense for the

concerned period; (3) the evaporation field is treated as error-free; and (4) the temporal variability is not affected to first order.

The experiment was started from rest on January 1, 1992 with the same initial conditions for temperature and salinity as long-DRAKKAR. The year 1992 was integrated three times before launching the interannual experiment over the 1993–2001 period.

2.3 Analyzes of the two simulations

In this study, we analyze the results from forced simulations without assimilation of observational data (e.g., altimetry or in situ data), contrary to what was done in other similar studies which used assimilative models (Carton et al. 2005; Wunsch et al. 2007; Köhl et al. 2007; Köhl and Stammer 2008). One of the goals of our study is to check whether these hindcasts correctly reproduce observed sea level and steric changes; they thus have to be totally independent of corresponding observational data. This approach is quite new for the study of sea level changes and puts on a further step toward accurate modeling and interpretation of future regional sea level change.

All results presented below are computed over the 1993–2001 common period, thus omitting 1992 as this is part of the spin-up in the short-MERCATOR simulation. Moreover, the T/P sea level observations used for comparison only begin in 1993. Model outputs (sea surface height [SSH], temperature, salinity, etc.) are provided as monthly means. We first compute annual means between 1993 and 2001, then trend maps over the period 1993–2001. As we focus on regional variations, a uniform mean trend has been removed from each map, and this will be the case for each regional trend map presented hereafter in this paper.

The choice of subtracting the globally averaged sea level trend throughout the paper is primarily driven by the objective of the present study which is a regional analysis. This choice is also required by the model itself: the Boussinesq approximation done in the primitive equations enforces the total ocean volume to remain constant, so that no global mean steric sea level signal can be inferred prognostically from the model sea level equations. The free surface evolution, however, mirrors the net freshwater surface flux in the model, both locally and in a globally integrated sense. Unlike evaporation which is computed online by bulk formulae, precipitation fields need to be prescribed, despite notable uncertainties due to rare observations. This also explains why the globally integrated sea level trend was subtracted in this study. It should be noted, however, that this simulated global trend remains very weak (around 6.4 mm/year) thanks to the well-balanced DRAKKAR forcing function. As shown by Greatbach (1994), apart from such unrealistic globally uniform rate of change, regional steric sea level changes are adequately represented in models that conserve volume rather than mass. Namely, regional redistribution of heat, salt, and water masses within the ocean by this kind of forced model allows diagnosing regional steric and mass sea level change. That is what we focus on hereafter.

3 Simulation of regional sea level change by the long-DRAKKAR model

3.1 Full regional sea level change: comparison model/observations

We first use SSH outputs from the long-DRAKKAR simulation to compute regional sea level trends between 1993 and 2001. Trends are computed at each grid point by fitting a line to the time series using least squares adjustment. Results are shown and compared to T/P-derived regional sea level trends (updated from Lombard et al. 2006) over the same period (Fig. 1). Local sea level trends are within the range ±35 mm/year over this period.

First, we note that the long-DRAKKAR simulation reproduces correctly the observed large-scale sea level trend patterns (see the map of temporal correlations on Fig. 2), especially the dipole-like pattern in the Pacific and Indian oceans linked to El Niño-southern oscillation (ENSO; we find a strong temporal correlation—above 0.7—between simulated SSH time series and the southern oscillation index (SOI) in large areas of the Pacific and Indian oceans), but also partly the patterns associated to the Pacific decadal oscillation (PDO) and North Atlantic oscillation (NAO) in the North Pacific and Atlantic oceans.

However, some large differences are also noticed (Fig. 3), especially in regions where sea level variability is strong like in the Antarctic circumpolar current (ACC), the Gulf Stream, and the Kurushio. This is not surprising as standard errors associated with the sea level linear trends computation are the largest (up to 35 mm/year) in the western boundary currents and ACC areas (Fig. 4). In addition, the sharp oceanic fronts in the Southern Ocean are not fully resolved in this eddy-admitting regime. In addition to model errors which are difficult to estimate, sea level trends deduced from T/P altimetry data are also impacted by errors at the regional scale (Ablain et al. 2008): this is especially due to uncertainties in the radiometer wet troposphere correction applied during the altimetry data processing which reaches 4 mm/year locally (wet areas) and to the orbit reference frame which is shown to have a strong hemispheric impact reaching 1 to 2 mm/year (Beckley et al. 2007).

Rigorously, part of these differences can also be explained by a somehow different physical content between

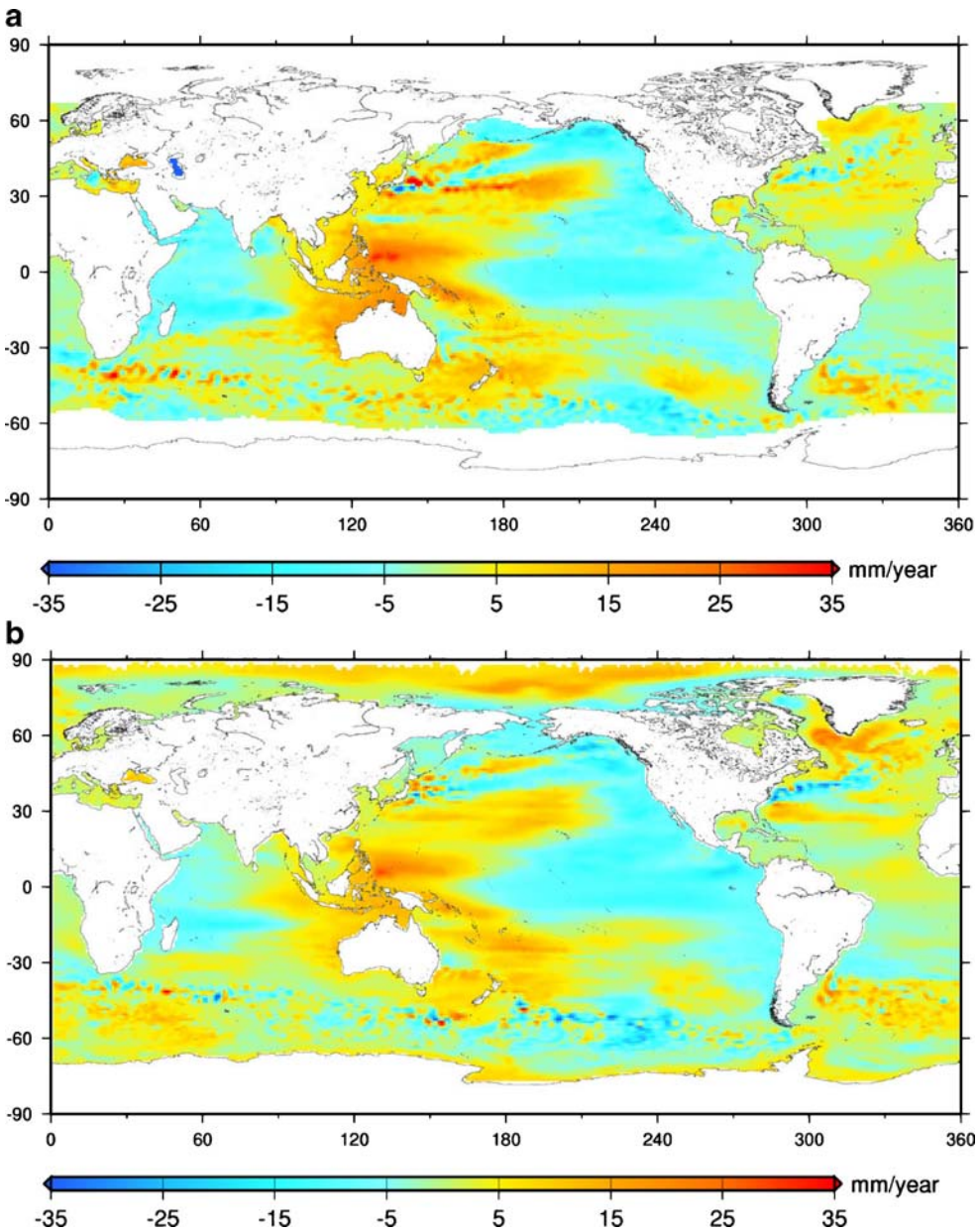

Fig. 1 Sea level trends between 1993 and 2001 from T/P altimetry data (**a**) and from the long-DRAKKAR simulation (**b**)

T/P observation and model simulation: glaciers and ice sheets melting, as well as land water change, are not included in the model (runoffs are climatologies). Moreover, regional footprint of glacial isostatic adjustment (GIA), as well as gravity effect due to land-ice melt, is not simulated in the model. However, the impact of these different processes on sea level change is supposed to be weak at the regional scale compared to other effects (e.g., steric effect, which can reach a few tenth of millimeters per year): GIA local impact is estimated to a few 0.1 mm/year (Peltier 2001, 2004), the same order of magnitude is found for self-gravitation local effect (Mitrovica et al. 2001; Plag and Juttner 2001; Plag 2006). A simulated weakening of the thermohaline circulation (THC) induced by a melting of Greenland ice sheet (GIS) is estimated by Levermann et al. (2005) to impact regional sea level at a rate reaching locally 20–25 mm/year. However, such a weakening of the THC directly linked to GIS melting has not yet been observed because natural multidecadal climate variability dominates the THC signal (Latif et al. 2006; Knight et al. 2005). Yet the impact of GIS melting on regional sea level trends through ocean circulation modification could be not negligible.

Altogether, the different processes not simulated in our model, but still present in T/P observations, seem to have a minor impact on regional sea level trends, but considering the uncertainties on misknown processes, one can not exclude locally significant contributions that would be observed by T/P and not present in the long-DRAKKAR model simulation. We keep that in mind along the paper

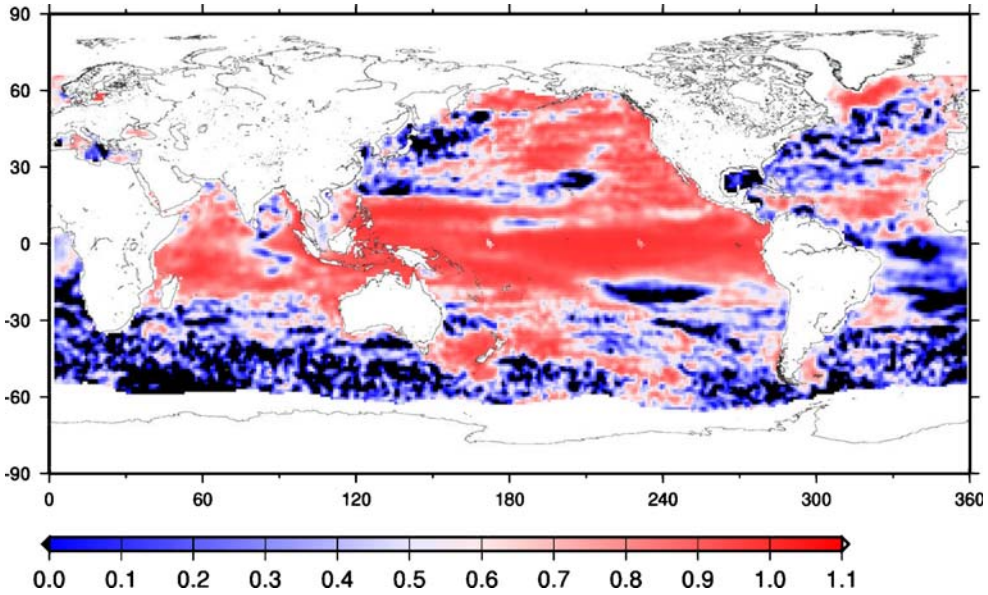

Fig. 2 Map of temporal correlation between T/P and the long-DRAKKAR simulation sea level time series

and recommend that these processes should be implemented in future model simulations.

A simple statistical analysis of the observation/model comparison is performed and presented in Table 1. The standard deviation σ of the sea level trends observed by T/P is computed over different regions, as well as the root mean square differences (hereafter, RMSD) of regional sea level trends between observations and model simulation. Basically, the larger the RMSD, the larger the mismatch between observation and simulation. In order to quantify this mismatch more objectively, we use a normalized RMSD (hereafter, NRMSD) which is computed as follows: NRMSD = RMSD/σ. NRMSD is expressed in percent, relative to the standard deviation of observations σ. In other terms, the NRMSD is X% of the standard deviation. As illustration, a NRMSD of 100% means that the gap between simulation and observation equals the observed standard deviation. A NRMSD lower than 100% is a good score, lower than 50% is excellent, whereas NRMSD greater than 100% reflect large differences between simulation and observation. Spatial correlations between observation and simulation are also indicated. All ocean basins are analyzed, zonal bands and global diagnostics are also given.

This analysis confirms that tropical Pacific and Indian ocean regional sea level trends are particularly well-simulated by the long-DRAKKAR model with NRMSD reaching, respectively, 47% and 49% (correlation with observations of 0.89 for both basins). On the contrary, southern Atlantic and Indian oceans as well as the northern Atlantic are poorly simulated, showing NRMSD of,

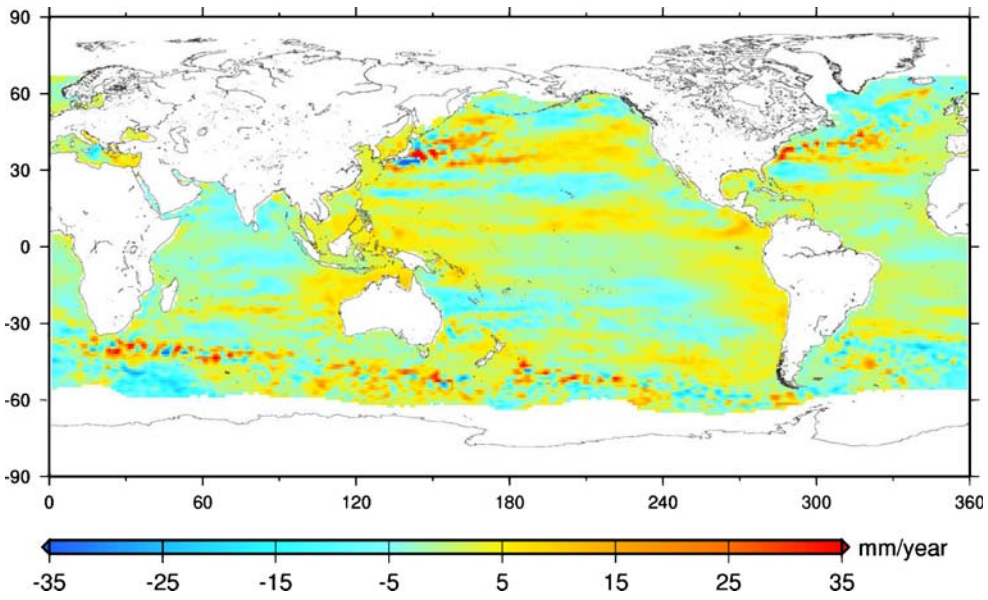

Fig. 3 Local differences between T/P and the long-DRAKKAR simulation sea level trends (Fig. 1a minus Fig. 1b)

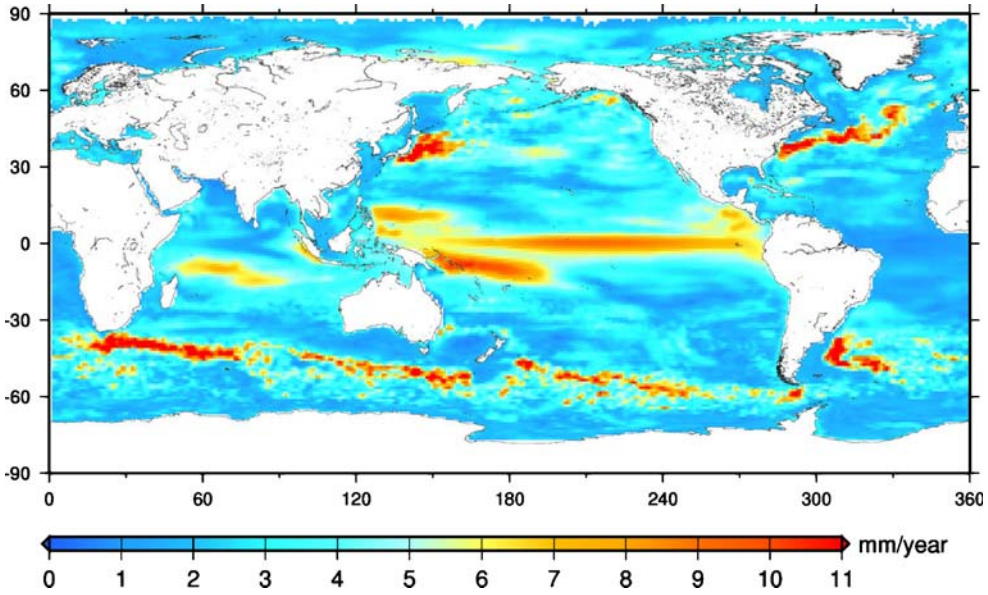

Fig. 4 Standard errors of sea level trends between 1993 and 2001 from the long-DRAKKAR simulation (Fig. 1b). In this study, we call "standard error" the estimated residual (or error) sum of squares that is computed under the simple linear regression model used to fit a slope (or trend) to sea level time series at each grid point

respectively, 101%, 116%, and 111% (correlation with observations of 0.39, −0.14, and 0.45). The other ocean basins (tropical Atlantic, southern Pacific, and northern Pacific) are correctly simulated with NRMSD of 95%, 84%, and 85% (correlation with observations of 0.55, 0.60, and 0.50), respectively. Globally, we find that regional sea level trends simulated by the long-DRAKKAR model are in very good agreement with T/P-derived observations (global NRMSD of 73%, correlation of 0.65), considering that there is no data assimilation.

Table 1 Spatial σ of sea level trends observed by T/P (first column), RMSD (NRMSD and spatial correlation indicated in parentheses) of sea level trends between T/P observations and long-DRAKKAR (second column)/short-MERCATOR (third column) simulations

	Observed T/P SSH σ [mm/year]	T/P—long-DRAKKAR RMSD, [mm/year (%)]	T/P—short-MERCATOR RMSD, [mm/year (%)]
Atlantic			
65S–65N	5.0	5.2 (104) (0.43)	8.5 (170) (0.06)
65S–30S	6.7	6.7 (101) (0.39)	13.2 (198) (−0.28)
30S–30N	2.5	2.4 (95) (0.55)	3.8 (148) (0.56)
30N–65N	5.7	6.3 (111) (0.45)	7.6 (133) (0.34)
Pacific			
65S–65N	8.7	5.9 (68) (0.73)	7.4 (85) (0.67)
65S–30S	7.4	6.2 (84) (0.60)	10.2 (139) (0.36)
30S–30N	8.3	3.9 (47) (0.89)	4.6 (55) (0.86)
30N–65N	11.5	9.7 (85) (0.50)	8.5 (73) (0.71)
Indian			
65S–65N	8.4	6.3 (74) (0.52)	10.1 (120) (0.36)
65S–30S	7.3	8.5 (116) (−0.14)	14.3 (195) (0.15)
30S–30N	7.6	3.8 (49) (0.89)	5.1 (67) (0.76)
Global			
65S–65N	7.9	5.8 (73) (0.65)	8.3 (105) (0.53)
65S–30S	7.2	7.0 (97) (0.39)	12.1 (168) (0.18)
30S–30N	7.3	3.6 (49) (0.87)	4.6 (63) (0.81)
30N–65N	10.2	8.3 (81) (0.48)	8.0 (78) (0.63)

3.2 Steric regional sea level change

Steric sea level is defined as the variation in sea level caused by the expansion/contraction of ocean volume due to density changes associated with temperature and salinity change in the water column (e.g., Patullo et al. 1955, Antonov et al. 2002, Lombard et al. 2006). Steric sea level is estimated by vertically integrating density anomalies, using the classical equation of state for sea water proposed by the United Nations Educational, Scientific and Cultural Organization (Gill 1982).

Steric sea level trends for 1993–2001 are computed using temperature (T) and salinity (S) outputs of the long-DRAKKAR simulation. T and S outputs are given on 46 levels from surface to bottom. As a result, we estimate—at each grid point—the total steric sea level change that is due to temperature variations as well as salinity variations in all layers from surface to bottom. It is worth noting that current estimates of steric sea level change based on in situ hydrographic observations are often limited to temperature effects and upper ocean layers down to 700 or 750 m only (Ishii et al. 2006; Lombard et al. 2006; Antonov et al. 2005; Willis et al. 2004). Until the recent deployment of Argo floats over the global ocean, salinity and deep temperature data were too sparse to be mapped globally (Roemmich et al. 1999).

As expected, the agreement between the regional steric sea level trend maps (Fig. 5) and the total sea level trend maps (Fig. 1b)—both computed using long-DRAKKAR model outputs—is very good (NRMSD between SSH and

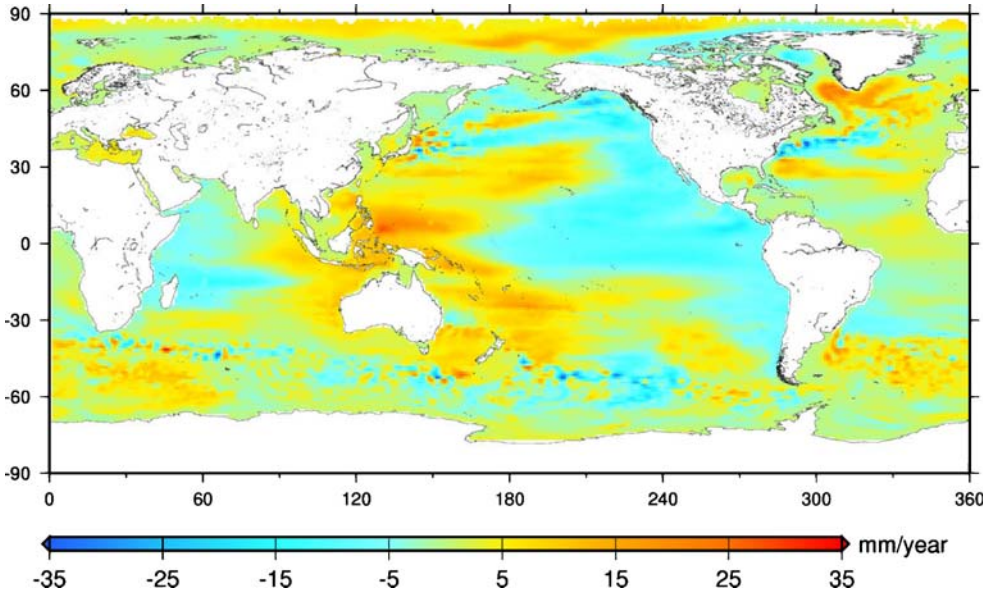

Fig. 5 Steric sea level trends between 1993 and 2001 from long-DRAKKAR *T* and *S* outputs

steric sea level trends of 22%). It seems that the model-derived regional sea level change distribution is almost totally governed by regional steric changes. However, we show below that some nonsteric (i.e., related to changes in mass, thus in bottom pressure) effects play a nonnegligible role in some parts of the ocean (see Section 3.3).

Steric sea level change can be split into its thermosteric (due to T change) and halosteric (due to S change) components (see, for example, Ishii et al. 2006; Antonov et al. 2002). Looking at the maps and at the RMSD in Table 2, it appears that thermosteric sea level change (Fig. 6—NRMSD of 58% globally) explains the major steric sea level change patterns (Fig. 5), especially in the Southern Ocean (NRMSD of 48%) and in the tropical oceans (NRMSD of 51%). This is not true for the Arctic Ocean (highest NRMSD of 89%) where steric sea level change is driven by halosteric changes.

However, the thermosteric signal (Fig. 6) is found to be stronger than the steric signal (Fig. 5) in some areas like the Atlantic Ocean and some parts of the Pacific Ocean where halosteric sea level change (Fig. 7) compensates thermosteric sea level change (Fig. 6). Such a mechanism is particularly obvious in the Atlantic Ocean. This has already been observed with in situ hydrographic data in the subpolar North Atlantic (Antonov et al. 2002; Levitus et al. 2005), in high latitudes, and the Atlantic Ocean (Ishii et al. 2006), as well as globally with assimilation models (Wunsch et al. 2007; Köhl et al. 2007; Köhl and Stammer 2008) and coupled climate model (Lowe and Gregory 2006). In some other areas, thermosteric and halosteric sea level change add up (main part of the Indian ocean, parts of the Southern Ocean, North–east Pacific). Finally, halosteric sea level change controls the Arctic Ocean's regional sea level patterns, while thermosteric sea level change appears uniformly positive there. Note that the relaxation of SSS performed throughout the simulation (see Section 2) may have introduced some artifacts in the computation of halosteric trends at high latitudes; however, considering the long relaxation time scales and the good agreement between simulated and observed SSH trends, there is probably no major contribution of SSS relaxation on trends.

In order to quantify the relationship between temperature and salinity contributions in terms of regional sea level change, we have computed the correlation coefficients between thermosteric and halosteric sea level time series at each grid point (Fig. 8). We find strong negative correlations (between −0.7 and −1) in the whole Atlantic, the South Pacific, and the South Indian ocean south of 25° S, except along the path of the ACC in all three oceans where the correlation is positive with some high values (between 0.7 and 1). The modeled and observed density-compensating changes (corresponding to negative correlations) that occur at large basin scales tend to preserve the local T–S relation, as an apparently typical behavior of the oceanic circulation change. Lowe and Gregory (2006)

Table 2 Spatial σ of steric sea level trends simulated by long-DRAKKAR model (first column) and RMSD (NRMSD indicated in parentheses) between steric sea level trends and thermosteric sea level trends (second column)

Long-DRAKKAR simulation	Steric σ [mm/year]	Steric–thermosteric RMSD, [mm/year (%)]
90S–30S	5.0	2.4 (48)
30S–30N	6.3	3.2 (51)
30N–60N	6.7	4.3 (64)
60N–90N	4.6	4.1 (89)
90S–90N	5.7	3.3 (58)

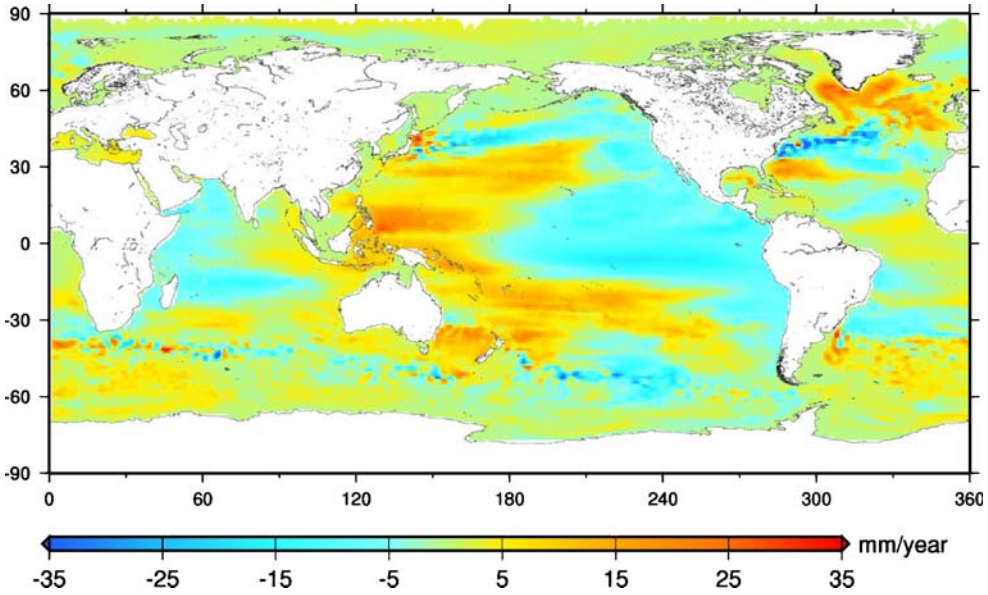

Fig. 6 Thermosteric (due to *T* change only) sea level trends between 1993 and 2001 from long-DRAKKAR *T* outputs

deduced that such compensation is not a property of climate change specifically but is widespread in the ocean, tending to reduce the range of density and the contrasts between adjacent water masses, for instance, across fronts. Wunsch et al. (2007) suggest that these compensating steric changes are due to adiabatic advection of water masses probably driven by wind stress. Our model results also seem to support the hypothesis that regional sea level changes result more from changes in the ocean circulation than in atmospheric heat and water fluxes.

In order to assess our model versus in situ observations, we compare the thermosteric sea level trends map computed using model *T* outputs for the upper 735 m (Fig. 9a) with thermosteric sea level trends computed from observational temperature data given for the upper 700 m (e.g., using Ishii et al. (2006) data set, Fig. 9b) over the same period 1993–2001. Table 3 sums up the results of the comparison in terms of RMSD between objectively mapped observations and model. The tropical oceans region is the closest to observations with a NRMSD of 68%. On the contrary, we find large discrepancies between the observed and simulated regional thermosteric sea level change in the Arctic (NRMSD of 121%) and Southern Oceans (NRMSD of 135%). This is not surprising as the sampling of in situ temperature observations in these remote oceans is poor, thus the "observed" signal is quite flat and may be nonsignificant (very small σ of 1.9 and 2.6 mm/year for Arctic/Southern Oceans, leading to large NRMSD). Finally, the northern

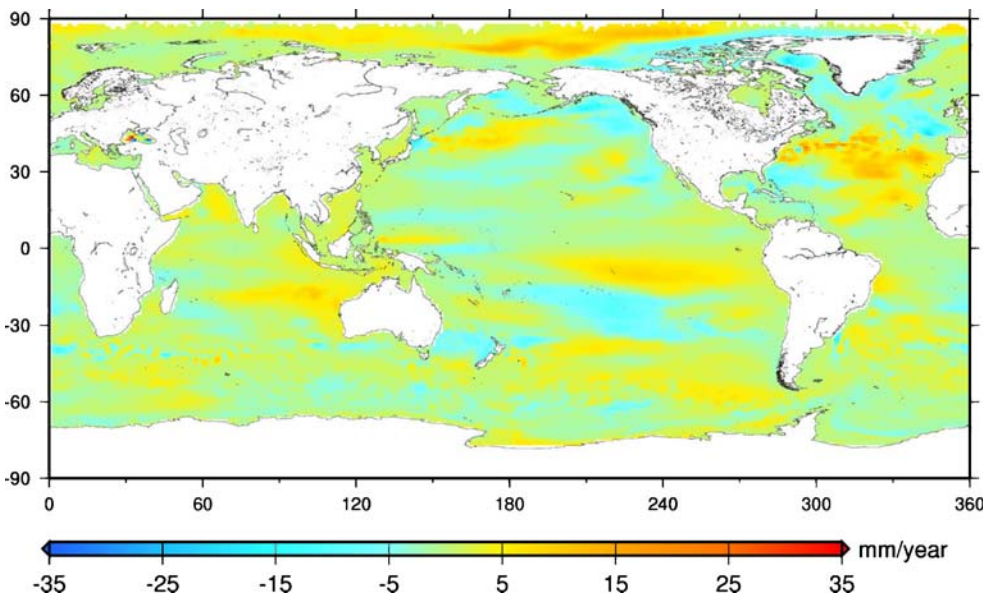

Fig. 7 Halosteric (due to *S* change only) sea level trends between 1993 and 2001 from long-DRAKKAR *S* outputs

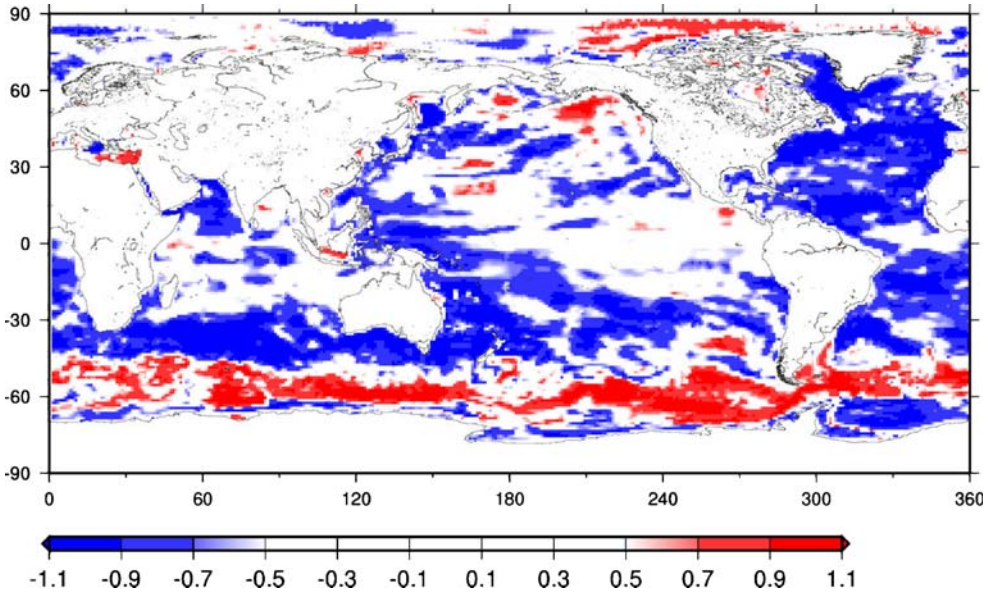

Fig. 8 Map of temporal correlation coefficients between thermosteric and halosteric sea level time series between 1993 and 2001 from long-DRAKKAR *T* and *S* outputs

oceans (30N–60N) present a surprisingly large statistical discrepancy between observation and model, considering the large amount of observational data in these regions (NRMSD of 124%). However, looking at the thermosteric trends maps (Fig. 9a, b) reveals similar regional patterns. Generally, the in situ observations-based trend map (Fig. 9b) presents weaker signals than the model-based maps (Fig. 9a). This is at least partly due to the large smoothing introduced during the objective analysis of the in situ data (Ishii et al. 2006) that can explain at least partly the discrepancy between model and observations in the northern oceans.

We have computed, respectively, the upper 0–735 m (Fig. 10a) and the deep 735-m bottom (Fig. 10b) contributions to regional steric sea level change. As can be seen on these maps, most of the regional steric sea level patterns (Fig. 5) are due to the upper 0–735 m layers (Fig. 10a). Table 4 confirms that, globally, the total steric sea level trend map is well-represented by the upper 0–735 m steric sea level trends map (NRMSD of 60%), especially in the tropical oceans (30S–30N) zone (NRMSD of 43%). However, the upper 0–735 m layers are less able to explain the total regional steric sea level trends in the Southern Ocean (90S–30S, NRMSD of 66%) as well as in the northern and Arctic oceans (30N–90N, NRMSD of 75%) where the deep 735-m bottom layers seem to contribute a lot (Fig. 10b).

Such a result has also been observed using in situ hydrographic data in the South Pacific subtropical gyre (Roemmich et al. 2007) and south of Australia (Morrow et al. 2007). Such strong sea level changes arising from deep layers in the Southern Ocean are attributed to frontal shifts due to large-scale changes in the wind forcing in relation with the atmosphere's southern annular mode (SAM) and ENSO variability (Sallee et al. 2008). In these high latitudes, the weak ocean stratification does not allow to separate upper layers from deep ocean, thus leading to a slow adjustment of the Southern Ocean.

However, we find that the observed regional sea level trends from T/P altimetry are better simulated by the model 0–735 m steric change (NRMSD of 68%) than by the full steric change (NRMSD of 75%). This result is shown in Table 5: the RMSD between observed regional sea level trends and modeled steric sea level trends is smaller when computing the steric sea level trends with only the upper 0–735 m layers of the ocean, especially in the Southern Ocean and in the Northern and Arctic oceans (tropical oceans are not affected). This result could mean that the contribution of deep layers steric sea level change to the full regional sea level change may not be correctly simulated by the model. As a consequence, we have to remain careful when interpreting the modeled deep layers contribution to total regional sea level change.

To summarize this part, model simulations indicate that most of the large-scale sea level change patterns are due to temperature change in the upper 750 m of the ocean. The contribution of salinity variations is still significant and should be taken into account in any regional sea level change study. Different studies that have analyzed the few in situ salinity data available reach the same conclusion (Delcroix et al. 2007).

The regional steric sea level changes simulated by the long-DRAKKAR model without data assimilation are in good agreement with the results of Carton et al. (2005) who analyzed the SODA1.2 ocean assimilation reanalysis and Wunsch et al. (2007), Köhl et al. (2007), and Köhl and Stammer (2008) who used different versions of the ECCO model with assimilation data over different periods.

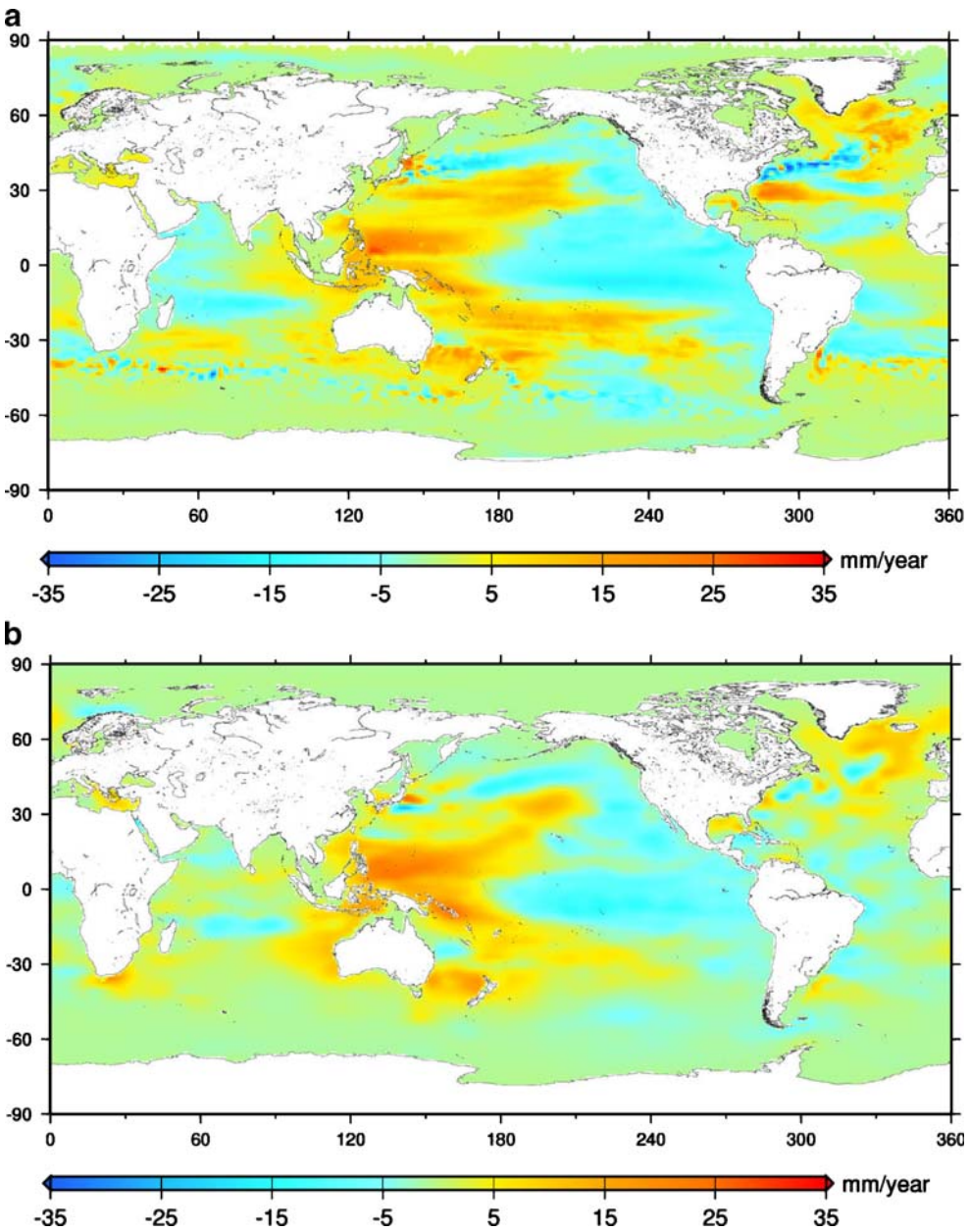

Fig. 9 Upper layers thermosteric sea level trends between 1993 and 2001 from long-DRAKKAR T (0–735 m) outputs (**a**) and from Ishii et al. (2006) 0–700 m T data (**b**)

Table 3 Spatial σ of thermosteric sea level trends deduced from in situ temperature observations of the upper 700 m objectively mapped by Ishii et al. (2006) (first column) and RMSD (NRMSD indicated in parentheses) of thermosteric sea level trends between Ishii et al. (2006) observations and long-DRAKKAR model (second column)

Thermosteric 0–750 m	Observed Ishii σ [mm/year]	Ishii—long-DRAKKAR RMSD, [mm/year, (%)]
90S–30S	2.6	3.5 (135)
30S–30N	6.3	4.3 (68)
30N–60N	5.4	6.7 (124)
60N–90N	1.9	2.3 (121)
90S–90N	4.6	4.2 (91)

3.3 Nonsteric regional sea level change

We have shown that regional sea level trends are almost totally due to regional steric sea level change, according to the long-DRAKKAR simulation. We check this by computing the residual sea level trend map (practically "SSH minus steric" sea level trends) using long-DRAKKAR SSH, T, and S outputs. As seen on Fig. 11, nonsteric (i.e., bottom pressure) sea level trends are generally weaker and more uniform than regional steric sea level trends (Fig. 5). However, local nonsteric effects are regionally important, for example, in the Southern Ocean (especially the Antarctic shelves and the South Pacific), the seas north of Australia, the Java Sea, around the Bering Strait, or in the Baffin Bay. Table 5 shows that taking into account the

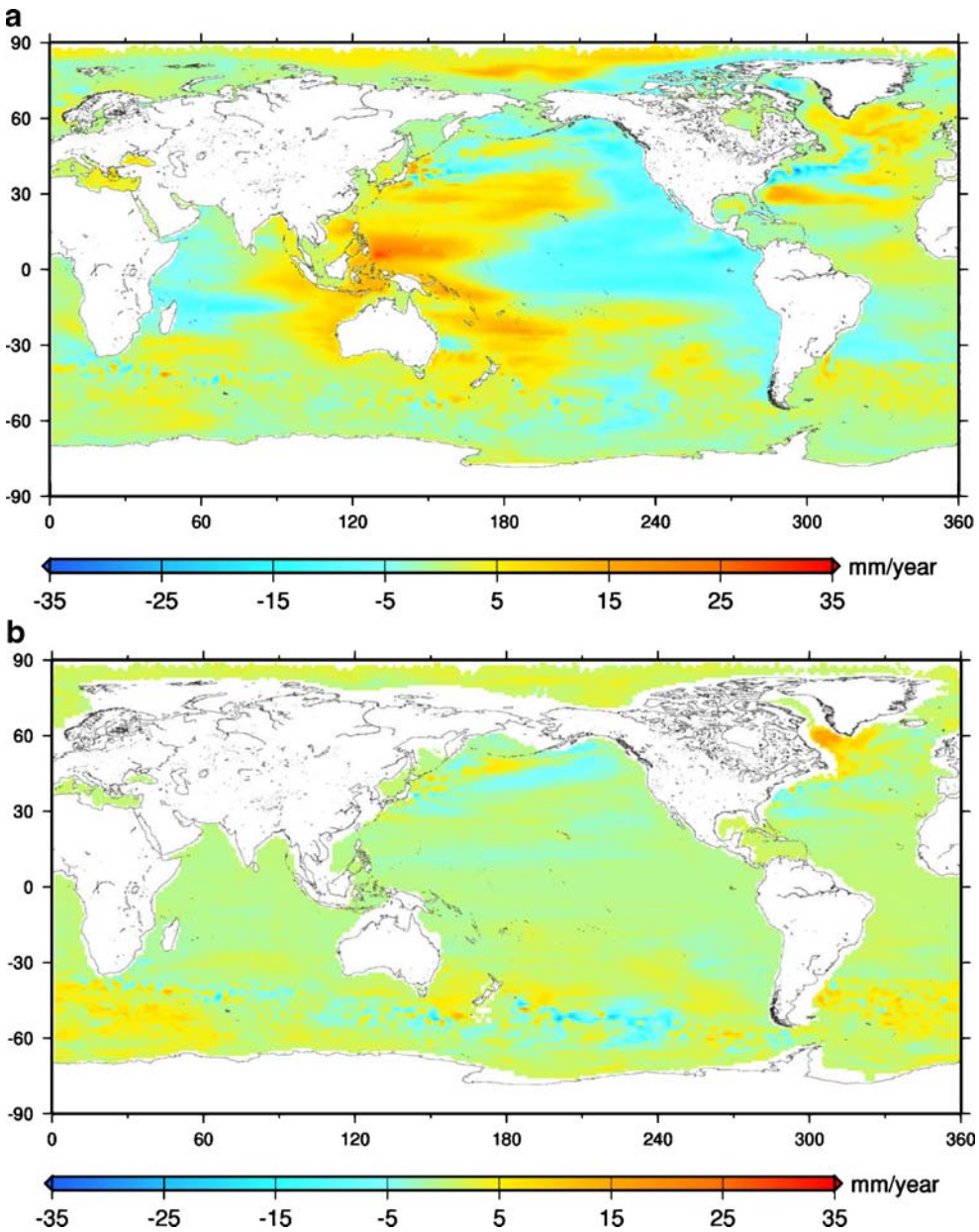

Fig. 10 0–735 m (**a**) and 735 m bottom (**b**) steric sea level trends between 1993 and 2001 from long-DRAKKAR *T* and *S* outputs

Table 4 Spatial σ of steric sea level trends computed using long-DRAKKAR *T* and *S* outputs (first column) and RMSD (NRMSD indicated in parentheses) of sea level trends between total steric and steric of the upper layers 0–735 m (second column) from long-DRAKKAR simulation

	Steric sea level trends σ [mm/year]	Steric—(steric 0–735 m) RMSD, [mm/year (%)]
90S–30S	5.0	3.3 (66)
30S–30N	6.3	2.7 (43)
30N–90N	5.7	4.3 (75)
90S–90N	5.7	3.4 (60)

bottom pressure regional changes, in addition to the upper layers steric regional sea level changes, does improve the agreement between observed and simulated regional sea level trends (global RMSD of 65% compared to 68%).

These nonsteric regional sea level changes correspond to regional bottom pressure changes caused by local changes in the mass of the water column. This can be due to a response to local atmospheric wind change, a redistribution of mass within the ocean through advection, or although unlikely, a regional change of the net water flux between atmosphere, land, and ocean (evaporation minus precipitation and runoff). In reality, other processes can also cause regional bottom pressure changes: for example, water mass addition from glaciers and ice sheets melting, runoff variations due to land water changes, changes in the ocean

Table 5 Spatial σ of sea level trends observed by T/P (first column) and RMSD (NRMSD indicated in parentheses) of sea level trends between T/P observations and long-DRAKKAR steric sea level trends (second column)/long-DRAKKAR upper ocean steric sea level trends (third column)/long-DRAKKAR upper ocean steric+bottom pressure sea level trends (fourth column)

	Observed T/P SSH σ [mm/year]	T/P—(steric) RMSD, [mm/year (%)]	T/P—(steric 0–735m) RMSD, [mm/year (%)]	T/P—(steric 0–735m+BP) RMSD, [mm/year (%)]
65S–30S	7.2	6.8 (94)	5.9 (82)	5.6 (78)
30S–30N	7.3	3.9 (53)	3.9 (53)	3.6 (49)
30N–65N	10.2	8.4 (82)	7.8 (76)	7.5 (74)
65S–65N	7.9	5.9 (75)	5.4 (68)	5.1 (65)

basin volume due to postglacial rebound, or gravity changes due to land-ice melt. However, as stated before, the latter effects are not taken into account in the model, so we do not discuss them in the present study.

We have analyzed water fluxes used as input forcings to the model but we find no evidence of a direct correlation between regional changes of net water fluxes and regional bottom pressure changes. This result is not very surprising, as local water mass input is redistributed very quickly by gravity. We find a high anticorrelation (around −0.9) between the SOI and some regional patterns of bottom pressure sea level trends, especially the strong positive patterns north of Australia and in the Java Sea.

Some regional patterns could also be explained by a simple redistribution model as shown by Landerer et al. (2007). For example, in the semiclosed seas, like the Mediterranean Sea, we note that a regional positive steric sea level trend is associated with a negative nonsteric (i.e., mass) sea level trend, and inversely for the Baffin Bay (negative steric trend, positive mass trend). This could be due to the horizontal gradient induced by the steric effect that causes a horizontal mass redistribution between the semiclosed area and the near ocean basin.

However, generally, the regional patterns of bottom pressure changes simulated by the model are quite difficult to interpret and we cannot assess whether they represent real signal or not. Anyway, there seems to be a correlation between regional bottom pressure changes and bathymetry. This remains to be investigated but is beyond the scope of the present study.

4 Comparison of long-DRAKKAR/short-MERCATOR model simulations

In order to assess the model sensitivity and robustness in terms of regional sea level trends, we compare here the long-DRAKKAR simulation to the short-MERCATOR simulation (common and different features between both presented in Section 2.). These two experiments differ by the length of the spin-up and the atmospheric forcing.

The short-MERCATOR regional sea level trends map is shown in Fig. 12. Short-MERCATOR statistical performances in terms of regional sea level trends simulation compared to T/P observations are added in Table 1 and can be directly compared to long-DRAKKAR performances (detailed in the

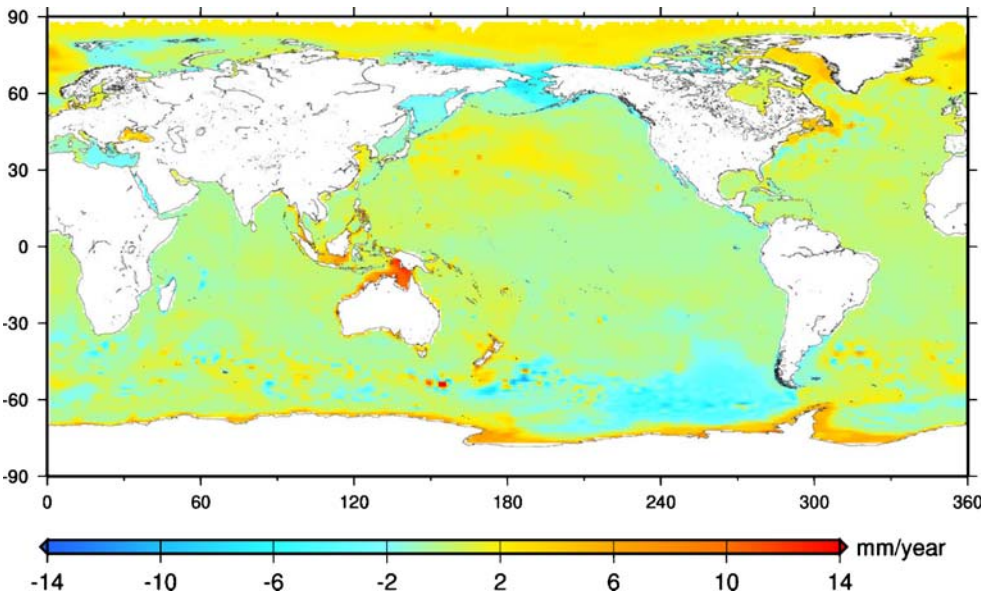

Fig. 11 Nonsteric (SSH minus steric, equivalent to bottom pressure) sea level trends between 1993 and 2001 from long-DRAKKAR SSH, *T*, and *S* outputs

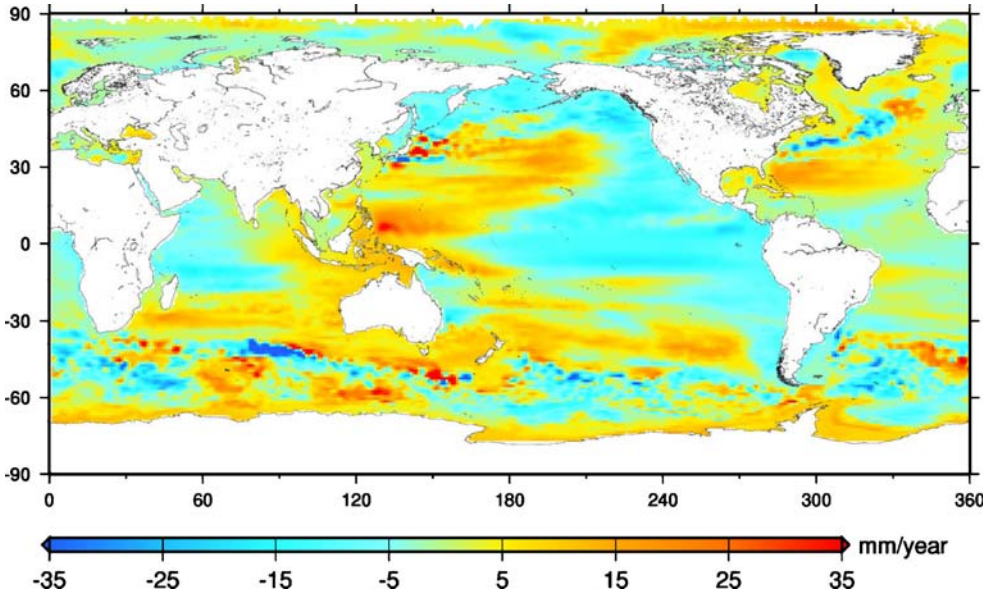

Fig. 12 Sea level trends between 1993 and 2001 from the short-MERCATOR simulation

Section 2 and shown on Fig. 1b). Except for the North Pacific basin, the long-DRAKKAR run performs globally better than the short-MERCATOR. However, the differences in terms of performance between both runs are not uniform.

First, the Southern Ocean is less realistic than in the long-DRAKKAR run (degradation of 71% of NRMSD), especially in the Atlantic sector (degradation of 97% of NRMSD). This problem may be attributed to the duration of the spin-up (34 years for long-DRAKKAR compared to 3 years for short-MERCATOR). Such a long period leaves time for adjustment by the long and slow waves produced at the time of initialization. This requirement is supported by the DRAKKAR Group (2007) who mentioned that more than 20 years of spin-up are necessary to stabilize the Southern Ocean stratification and the ACC transport in simulations of this kind. This explanation is particularly relevant as long-DRAKKAR and short-MERCATOR use the same wind product, e.g., the ERA40 dataset.

Accordingly, the tropical oceans, which adjust more quickly, are quite well-simulated in the short-MERCATOR (NRMSD of 63%, correlation with observations of 0.81), especially in the tropical Pacific (improvement of only 8% of NRMSD in the long-DRAKKAR run). Finally, we find that the northern Pacific is slightly better simulated in the short-MERCATOR run than in the long-DRAKKAR run (12% of NRMSD improvement). This later result would mean that, at least in the tropical and northern Pacific, the length of the spin-up is not an issue, a realistic adjustment of water masses being quickly reached in the model driven by the surface forcing.

The difference map (Fig. 13) of regional sea level trends between the long-DRAKKAR and short-MERCATOR simulations reveals strongest differences at high latitudes. We investigate the origin of these regional differences through a statistical analysis summed up in Table 6. Sea level trends differences are mostly explained by upper layer steric contributions, except for the Southern Ocean where the contribution of deep layers steric effects dominate (smaller NRMSD with total SSH differences of 55% compared to 60% for the upper layers). This latest result confirms the need for a long spin-up to adjust deep water masses in the Southern Ocean. Differences between both simulations mainly come from thermosteric differences, except in the Arctic Ocean where the contribution of halosteric differences dominates (smaller NRMSD with total SSH differences of 52% compared to 94% for the thermosteric component). A more detailed analysis (not shown here) reveals that these halosteric differences are confined in the upper layers. The strong difference in upper layers halosteric sea level trends between both simulations in the Arctic may be due to different surface forcings, but we cannot exclude the contribution of spin-up length. The different SSS relaxation time scales between both simulations (mainly under sea-ice, see Section 2) could also explain some of the differences at high latitudes. In any case, assessing either simulation in the Arctic Ocean in terms of sea level trends is very difficult, as no T/P observation data is available beyond 66°.

Overall, the comparison between long-DRAKKAR and short-MERCATOR simulations ability in reproducing regional sea level trends shows that:

- the spin-up length is very important in particular regions like the Southern Oceans (need for a few decades spin-up);
- the spin-up length is not a crucial parameter for tropical (30S–30N) and northern (30N–60N) ocean basins;
- part of the better performance of long-DRAKKAR may also be attributed to the DFS3 hybrid surface forcing; and

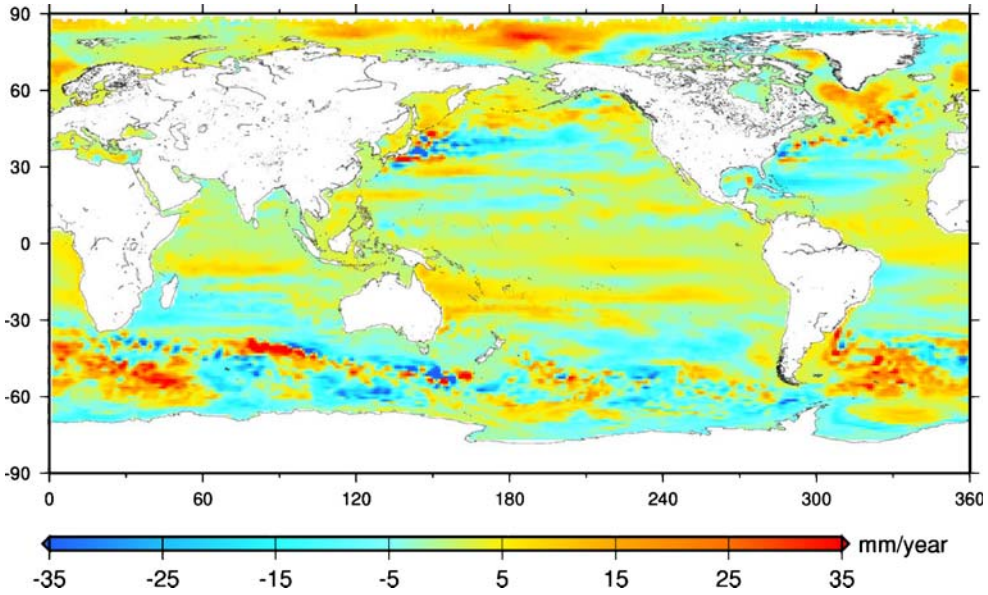

Fig. 13 Difference map of sea level trends between 1993 and 2001 from the long-DRAKKAR minus short-MERCATOR simulations (Fig. 1b minus Fig. 12)

- the ERA40 atmospheric forcing (which is the core of both surface forcing data sets) appears quite pertinent for this kind of study.

5 Discussion and conclusions

In this study, we use a global ocean model at 1/4° resolution, driven by atmospheric forcing but without any data assimilation to examine spatial patterns of sea level change. Our first goal is to quantify how well such models reproduce altimeter observations, as this has never been done before (previous similar studies used assimilation models). We find that this model simulates well the large-scale patterns of sea level change as observed by satellite altimetry (T/P) over 1993–2001. Probably due to a better atmospheric forcing and a longer spin-up, the long-DRAKKAR experiment yields better results with a RMSD with observations 30% smaller than the short-MERCATOR experiment. In particular, it appears that a spin-up of a few decades is needed to adjust the Southern Ocean. The CORE forcing used in long-DRAKKAR for the computation of radiative fluxes and precipitations (instead of ERA40) may also contribute to the better performance of long-DRAKKAR compared to short-MERCATOR. As a result, we recommend the use of long-DRAKKAR-like model simulations with long spin-up for future studies on spatial patterns of sea level change.

The second goal of this study is to provide a physical insight into the mechanisms of regional sea level change. We examine the respective contributions of steric and mass changes, thermosteric and halosteric changes, and upper ocean and lower ocean steric changes. We find that regional sea level change is mainly due to regional thermosteric change within the upper 750 m. This result confirms earlier studies based on in situ temperature data and satellite altimetry observations, as well as other model-based studies. Salinity variations are found to have a substantial

Table 6 Spatial σ of the difference between long-DRAKKAR and short-MERCATOR sea level SSH trends (first column), RMSD (NRMSD indicated in parentheses) between SSH difference and, respectively, upper layer steric difference (second column), deep layer steric difference (third column), thermosteric difference (fourth column), and halosteric difference (fifth column)

Diff. = long-DRAKKAR minus short-MERCATOR differences	SSH diff. σ [mm/year]	SSH diff.–steric 0–735 m diff. RMSD, [mm/year (%)]	SSH diff.–steric 735 m bottom diff. RMSD, [mm/year (%)]	SSH diff.–thermosteric diff. RMSD, [mm/year (%)]	SSH diff.–halosteric diff. RMSD, [mm/year (%)]
90S–30S	12.0	7.2 (60)	6.7 (55)	6.3 (52)	11.4 (94)
30S–30N	4.7	1.3 (27)	4.1 (87)	3.7 (78)	5.8 (122)
30N–60N	9.9	4.1 (41)	8.1 (82)	6.8 (68)	11.9 (120)
60N–90N	7.1	3.9 (54)	9.1 (128)	8.3 (117)	3.7 (51)
90S–90N	8.8	4.8 (54)	6.3 (70)	5.9 (67)	8.7 (99)

impact on steric sea level change in some regions, especially in the Arctic and the Atlantic Ocean where they either enhance or moderate the thermosteric effect. Globally, taking into account salinity variations into the computation of steric sea level brings a 15% improvement in terms of RMSD with regional sea level trends observations. In addition, the deep ocean (below 750 m) contribution to steric sea level change seems to play a large role, especially in high latitude areas; the latter result needs to be considered with caution, as we find a poorer agreement (10% deterioration of RMSD) with observations when taking into account deep ocean layers into the computation of steric sea level change.

Analyzing our long-DRAKKAR experiment over the longer 47-year period (1958–2004) will also be necessary in order to check whether the last decade sea level trends are stationary or not and to investigate what are the dominant forcing factors on the longer-term. A recent study by Köhl and Stammer (2008) use the GECCO synthesis (ECCO/MIT ocean circulation model assimilating all in situ and satellite observations that were collected since the 1950s) to estimate regional sea level change over the 40-year period 1962–2001 and the 11-year period 1992–2002. They show that, over the period 1962–2001, most of the SSH changes are caused by changes in wind stress and associated barotropic stream function, whereas over the last decade, surface heat and freshwater fluxes contribute significantly (up to 50%) to sea level trends, especially in the northern hemisphere and the ACC region.

Our regional nonsteric (mass) sea level change map exhibits spatial structures with a large-scale more uniform pattern but showing locally some strong contributions. Such a nonsteric sea level trend map has never been produced from observational data because no global bottom pressure observations were available. Now, with the observations of the GRACE gravity mission (Tapley et al. 2004), we have access to the spatiotemporal changes of water masses, thus to the nonsteric part of sea level changes. Although the signals we will look for are quite small and might be sometimes lost in the leakage of surrounding land water changes, we think that we will be able in the near future to map locally observed bottom pressure changes and thus to validate these model outputs. In addition, our present model does not take into account the runoff changes linked to glaciers and ice sheets mass changes, as well as land water changes, so our modeled bottom pressure change map cannot be fully realistic.

Our study shows that a nonassimilative accurate general ocean circulation model driven by carefully calibrated wind and buoyancy forcing can realistically simulate observed regional sea level changes. Even without data assimilation, our long-DRAKKAR model seems to perform as well as assimilative models like ECCO (Köhl and Stammer 2008) or SODA (Carton et al. 2005), at least for large-scale and slow sea level change patterns driven by surface fluxes. As a result, we do not see any major drawback of using such nonassimilative models for any study of regional interannual sea level changes. We suggest that such models should be considered for future predictions of regional sea level changes. For further regional sea level change studies, we also recommend to implement a more realistic model experiment that simulates local runoff interannual changes (at least a trend) based on observed glacier melting (e.g., Dyurgerov and Meier 2005; Kaser et al. 2006 for a summary and complete references), ice sheets melting (e.g., Cazenave 2006 or Sheperd and Wingham 2007 for a summary and complete references), and hydrological basin land water storage changes (e.g., Ramillien et al. 2008).

Acknowledgements This study was carried out under the support of the Groupe Mission Mercator Coriolis (GMMC), and one of us (AL) benefited from a CNES postdoc grant. Computations for the short-MERCATOR experiment were performed on the IBM SP4 of the European Centre for Medium-Range Weather Forecasts. Support to DRAKKAR comes from various grants and programs listed hereafter: French national programs GMMC, PATOM, and PNEDC; PICS 2475 from Institut National des Sciences de l'Univers (INSU) and Centre National de la Recherche Scientifique (CNRS); Kiel SFB460 and CLIVAR-marin (03F0377A/B) supported by Deutsche Forschungsgemeinschaft. Computations for the long-DRAKKAR experiment were performed at Institut du Développement et des Ressources en Informatique Scientifique (IDRIS). Partial support from the European Commission under Contract SIP3-CT-2003-502885 (MERSEA project) is gratefully acknowledged. We thank Jean-Marc Molines for providing the DRAKKAR data and Anny Cazenave for the helpful comments. We thank the two reviewers for their thorough reviews which led to significant improvement of the manuscript.

References

Ablain M, Cazenave A, Do Minh K, Valladeau G, Guinehut S (2008) A new assessment of global mean sea level from altimeters highlights a reduction of global trend from 2005 to 2008. Ocean Sciences (in press)

Adcroft A, Hill C, Marshall J (1997) Representation of topography by shaved cells in a height coordinate ocean model. Mon Weather Rev 125:2293–2315, doi:10.1175/1520-0493(1997)125<2293:ROTBSC>2.0.CO;2

Antonov JI, Levitus S, Boyer TP (2002) Steric sea level variations during 1957–1994: importance of salinity. J Geophys Res 107 (C12):8013, doi:10.1029/2001JC000964

Antonov JI, Levitus S, Boyer T (2005) Steric variability of the world ocean, 1955–2003. Geophys Res Lett 32(12):L12602, doi:10.1029/2005GL023112

Barnier B, Madec G, Penduff T, Molines J-M, Treguier A-M, Le Sommer J, Beckmann A, Biastoch A, Böning C, Dengg J, Derval C, Durand E, Gulev S, Remy E, Talandier C, Theetten S, Maltrud M, McClean J, De Cuevas B (2006) Impact of partial steps and momentum advection schemes in a global ocean circulation model at eddy-permitting resolution. Ocean Dyn 56:543–567, doi:10.1007/s10236-006-0082-1

Beckley BD, Lemoine FG, Luthcke SB, Ray RD, Zelensky NP (2007) A reassessment of global and regional mean sea level

trends from Topex and Jason-1 altimetry based on revised reference frame and orbits. Geophys Res Lett 34:L14608, doi:1029/2007GL030002

Brodeau L, Barnier B, Penduff T, Treguier AM, Gulev SK (2007) An ERA40-based atmospheric forcing for global ocean circulation models. Ocean Modelling (in revision)

Cabanes C, Cazenave A, Le Provost C (2001) Sea level change from Topex/Poseidon altimetry for 1993–1999 and possible warming of the southern oceans. Geophys Res Lett 28(1):9–12, doi:10.1029/2000GL011962

Carton JA, Giese BS, Grodsky SA (2005) Sea level rise and the warming of the oceans in the Simple Ocean Data Assimilation (SODA) ocean reanalysis. J Geophys Res 110:C09006, doi:10.1029/2004JC002817

Cazenave A (2006) How fast are Greenland and Antarctica loosing ice mass. Science 314:1250–1252, doi:10.1126/science.1133325

Dai A, Trenberth KE (2002) Estimates of freshwater discharge from continents: latitudinal and seasonal variations. J Hydrometeorology 3:660–687

Delcroix T, Cravatte S, McPhaden MJ (2007) Decadal variations and trends in tropical Pacific sea surface salinity since 1970. J Geophys Res 12:C03012, doi:10.1029/2006JC003801

DRAKKAR Group (2007) Eddy-permitting ocean circulation hindcasts of past decades. CLIVAR Exchanges 12(3):8–10

Dyurgerov M, Meier MF (2005) Glaciers and changing Earth system: a 2004 snapshot. INSTAAR, Boulder, CO

Fichefet T, Maqueda MAM (1997) Sensitivity of a global sea ice model to the treatment of ice thermodynamics and dynamics. J Geophys Res 102(C6):12609–12646

Gill AE (1982) Atmosphere-ocean dynamics. Academic Press, San Diego, Calif., 662 pp

Goose H, Fichefet T (1999) Importance of ice-ocean interactions for the global ocean circulation: a model study. J Geophys Res 104:23337–23355

Goose H, Campin J-M, Deleersnijder E, Fichefet T, Mathieu P-P et al (2001) Description of the CLIO model version 3.0. Institut d'Astronomie et de Géophysoque Georges Lemaitre, Catholic University of Louvain, Belgium

Greatbach RJ (1994) A note on the representation of steric sea level in models that conserve lume rather than mass. J Geophys Res 99 (C6):12,767–12,771, doi:10.1029/94JC00847

Guinehut S, Le Traon PY, Larnicol G, Philipps S (2004) Combining Argo and remote-sensing data to estimate the ocean three dimensional temperature fields—a first approach based on simulated observations. J Mar Syst 46:85–98, doi:10.1016/j.jmarsys.2003.11.022

Huffman GJ, Arkin PA, Chang A, Ferraro R, Gruber A, Janowiak JE, Joyce RJ, McNab A, Rudolf B, Schneider U, Xie P (1997) The Global Precipitation Climatology Project (GPCP) Combined Precipitation Data Set. Bull Am Meteorol Soc 78:5–20, doi:10.1175/1520-0477(1997)078<0005:TGPCPG>2.0.CO;2

Ishii M, Kimoto M, Sakamoto K, Iwasaki SI (2006) Steric sea level changes estimated from historical ocean subsurface temperature and salinity analyses. J Oceanogr 62(2):155–170, doi:10.1007/s10872-006-0041-y

Kaser G, Cogley JG, Dyurgerov MB, Meier MF, Ohmura A (2006) Mass balance of glaciers and ice caps: consensus estimates for 1961–2004. Geophys Res Lett 33:L19501, doi:10.1029/2006GL027511

Knight JR et al (2005) A signature of persistent natural thermohaline circulation cycles in bserved climate. Geophys Res Lett 32: L20708, doi:1029/2005GL024233

Köhl A, Stammer D (2008) Decadal Sea Level Changes in the 50-Year GECCO Ocean Synthesis. J Clim 21:1876–1890, doi:10.1175/2007JCLI2081.1

Köhl A, Stammer D, Cornuelle B (2007) Interannual to decadal changes in the ECCO global synthesis. J Phys Oceanogr 37 (2):313–337, doi:10.1175/JPO3014.1

Landerer FW, Jungclaus JH, Marotzke J (2007) Ocean bottom pressure changes lead to a decreasing length-of-day in a warming climate. Geophys Res Lett 34:L06307, doi:10.1029/2006GL029106

Latif M et al (2006) Is the thermohaline circulation changing? J Clim 19:4631–4637, doi:10.1175/JCLI3876.1

Large WG, Yeager SG (2004) Diurnal to decadal global forcing for ocean and sea-ice models: The data sets and flux climatologies. Technical Report TN-460+STR, NCAR, 105 pp

Levermann A, Griesel A, Hofmann M, Montoya M, Rahmstorf S (2005) Dynamic sea level changes following changes in the thermohaline circulation. Clim Dyn 24:347–354, doi:10.1007/s00382-004-0505-y

Levitus S, Antonov J, Boyer T (2005) Warming of the World Ocean, 1955–2003. Geophys Res Lett 32:L02604, doi:10.1029/2004GL021592

Lombard A, Cazenave A, Le Traon PY, Guinehut S, Cabanes C (2006) Perspectives on present-day sea level change: a tribute to Christian Le Provost. Ocean Dyn 56:445–451, doi:10.1007/s10236-005-0046-x

Lowe JA, Gregory JM (2006) Understanding projections of sea level rise in a Hadley Centre coupled climate model. J Geophys Res 111:C11014, doi:10.1029/2005JC003421

Madec G, Delecluse P, Imbard M, Levy C (1998) OPA 8.1 general circulation model reference manual. Notes de l'IPSL, University P. et M. Curie, B102 T15-E5, 4 place Jussieu, Paris cedex 5, No. 11, p 91

Mathiot P, Barnier B, Gallée H, Molines JM, Penduff T (2007) Correction of katabatic winds in ERA40 and its effect on polynya and shelf water in Antarctica. Geophys Res Abstr 9:02795 (SRef-ID: 1607-7962/gra/EGU2007-A-02795)

Mitrovica JX, Tamisiea M, Davis JL, Milne GA (2001) Recent mass balance of polar ice sheets inferred from patterns of global sea-level change. Nature 409:1026–1029, doi:10.1038/35059054

Morrow R, Valladeau G, Sallee JB (2007) Observed subsurface signature of Southern Ocean sea level rise. Prog Oceanogr 77:351–366

Patullo JG, Munk WH, Revelle R, Strong E (1955) The seasonal oscillation of sea level. J Mar Res 14:88–156

Peltier WR (2001) Global glacial isostatic adjustment and modern instrumental records of relative sea level history. In: Douglas BC, Kearney MS, Leatherman SP (eds) Sea level rise: history and consequences. Academic, San Diego, pp 65–95

Peltier WR (2004) Global glacial isostasy and the surface of the ice-age earth: the ICE-5G (VM2) model and GRACE. Annu Rev Earth Planet Sci 32:111–149, doi:10.1146/annurev.earth.32.082503.144359

Plag H-P (2006) Recent relative sea level trends: an attempt to quantify the forcing factors. Phil Trans Roy Soc London 364:821–844, doi:10.1098/rsta.2006.1739

Plag H-P, Juttner H-U (2001) Inversion of global tide gauge data for present-day ice load changes. Proceedings of the Second International Symposium on Environmental Research in the Arctic and Fifth Ny-Alesund Scientific Seminar, Mem Natl Instl Polar Res, pp 301–318

Ramillien G, Bouhours S, Lombard A, Cazenave A, Flechtner F, Schmidt R (2008) Land water storage contribution to sea level from GRACE geoid data over 2003–2006. Global Planet Change 60:381–392, doi:10.1016/j.gloplacha.2007.04.002

Roemmich D, Boebel O, Desaubies Y, Freeland H, King B, Le Traon P-Y, Milinari B, Owens B, Riser S, Send U, Takeuchi K, Wijffels S (1999) Argo: the global array of profiling floats. Proceedings of the Ocean Observing System for Climate, International Symposium, Saint Raphaël, France

Roemmich D, Gilson J, Davis R, Sutton P, Wijffels S, Riser S (2007) Decadal spin-up of the South Pacific subtropical gyre. J Phys Oceanogr 37(2):162–173, doi:10.1175/JPO3004.1

Sallee JB, Speer K, Morrow RA (2008) Ocean fronts and their variability to climate modes. J Clim 21(2):3020–3039

Sheperd A, Wingham D (2007) Recent sea level contributions of the Antarctic and Greenland ice sheets. Science 315:1529, doi:10.1126/science.1136776

Tapley BD, Bettadpur S, Watkins M, Reigber C (2004) The gravity recovery and climate experiment: mission overview and early results. Geophys Res Lett 31:L09607, doi:10.1029/2004GL019920

Willis JK, Roemmich D, Cornuelle B (2004) Interannual variability in upper-ocean heat content, temperature and thermosteric expansion on global scales. J Geophys Res 109:C12036, doi:10.1029/2003JC002260

Wunsch C, Ponte RM, Heimbach P (2007) Decadal trends in sea level patterns:1993–2004. J Clim 20:5889–5911, doi:10.1175/2007JCLI1840.1